ECS Transactions, 50 (6) 55-60 (2012)
10.1149/05006.0055ecst ©The Electrochemical Society

One-Dimensional Semiconductor Heterostructures: Challenges and Opportunities

S. A. Dayeh

Center for Integrated Nanotechnologies, Los Alamos National Laboratory, Los Alamos, NM 87111

The boundary conditions for materials science and device physics in 1D semiconductors are dramatically different from their bulk counterparts. From a materials perspective, surface energetics dominates growth and structural integrity in 1D materials and helps extend their coherency limits for heterostructuring compared to bulk. From a device perspective, compositional changes along their 1D axis provide new control over charge transport, and their cylindrical structure allows for better electronic and optoelectronic device architectures. While we exploited interface engineering to provide new foundations for materials science in nanoscale 1D semiconductors and to perfect their crystal growth, we highlight below some of the opportunities made available by such advances and discuss the challenges that face their development a fundamental growth-device inter-relation level. We focus our discussion on bottom-up or vapor-liquid-solid 1D grown Ge/Si heterostructures.

Axial 1D Heterostructures

One of the most fascinating aspects of the vapor-liquid-solid (VLS) growth of 1D semiconductor nanowires (NWs) is the ability to change composition along their axis, thereby allowing additional control along the carrier transport direction through axial band-gap engineering. In contrast to traditional liquid phase epitaxy, VLS growth of NWs with sub-100 nm diameters allows aggressive composition modulation along their axis with anticipated defect free structures (1). Around the time of the birth of the VLS growth (2), several reports have discussed Ge-Si whisker growth up to a 45% composition ratio and pointed out that such structures can be used for benefiting from properties of both semiconductors (3). The topic of axial 1D heterostructures regained momentum with the reports of Wu et al. on Ge-Si axial superlattices with 12% composition modulation in 2002 (4). One of the challenging aspects in the Ge-Si axial NW growth is the stability of the Au growth seed, which deteriorates as the growth species (and growth temperatures) are switched in the growth reactor. We developed a growth sequence that enabled stability of the Au growth seed and 100 % composition modulated Ge-Si axial NWs with single crystal character (5). However, such growth doesn't come without any compromises. We discuss below these compromises and some unique device examples that are enabled by such 1D heterostructuring.

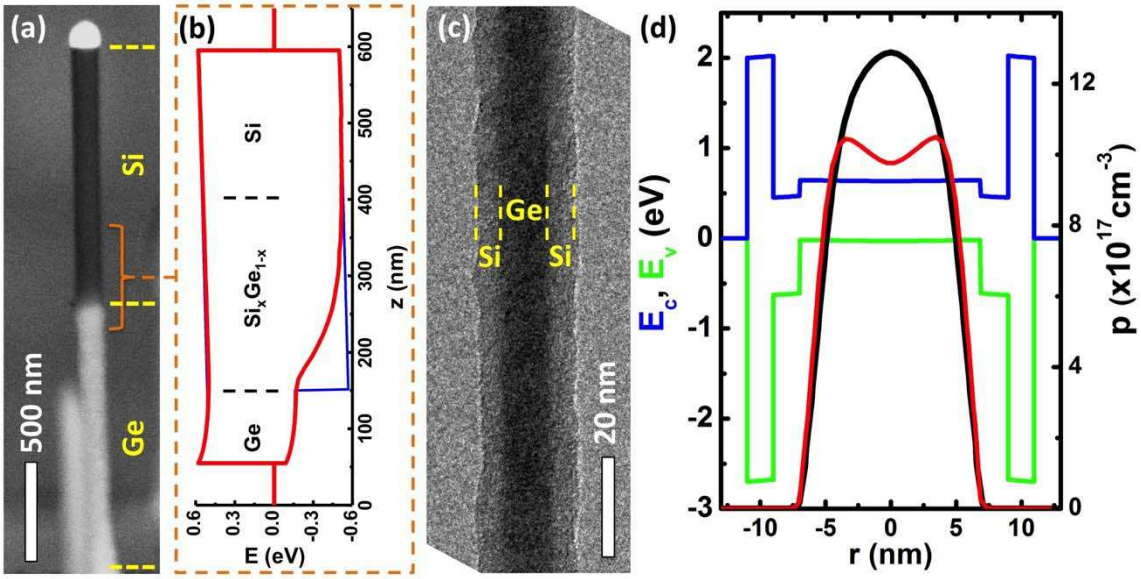

Figure 1. (a) Back scattering electron microscope image of a Ge (bright) – Si (dark) axial heterostructures NW with 100 % composition modulation. (b) Energy band-edge profile near the interface of Ge-Si NW calculated based on experimental compositional modulation data on a 20 nm diameter NW (ref. [5]), showing a graded transition in the valence band energy with a 'gradient tail' that extends a few 100 nms (red profile) and contrasted to the case of an abrupt Ge-Si axial junction. (c) Transmission electron microscope image of a radial Ge/Si heterostrucutre NW and (d) correspondent band-diagram assuming a surrounding dielectric shell showing hole confinement at the center of the Ge core (thick black line) or near the Ge/Si interface by Ge shell doping (thin red line).

Challenges.

While the 100% composition modulation in axial Ge/Si NWs has recently been achieved (5), the graded composition interface represents an obstacle for using such heterostructures in meaningful device applications that can truly benefit from the hetero-interface. This situation is illustrated in Figure 1 (a) where obvious intermixing occurs at the Ge-Si interface, and a graded energy band-edge diagram results as illustrated in Fig. 1 (b). This graded valence band energy profile utilizes experimentally measured compositional profiles on a 20 nm diameter Ge-Si axial NW heterostructure (5) without background doping, and is contrasted to that of an abrupt heterostructures band-edge profile. The long axial graded valence band profile represents specifically two main obstacles from an electronic device perspective: (i) devices that aim to utilize tunneling at the heterointerface are not be possible, i.e. tunneling processes are likely to occur in one material but not across the heterointerface between two materials and (ii) scaling of any devices that use such graded valence band profiles will not have large composition changes. Recent progress on alloyed growth seeds may allow slightly sharper interfaces (by ~ 4X) with some compromises of depositing alloy particulates on the NW surface or growth of extra sidewall whiskers (6). Interface abruptness down to the single nanometer scale level will be hard to achieve with VLS, and control over doping and composition changes in a liquid growth seed further reinforces the abruptness challenge.

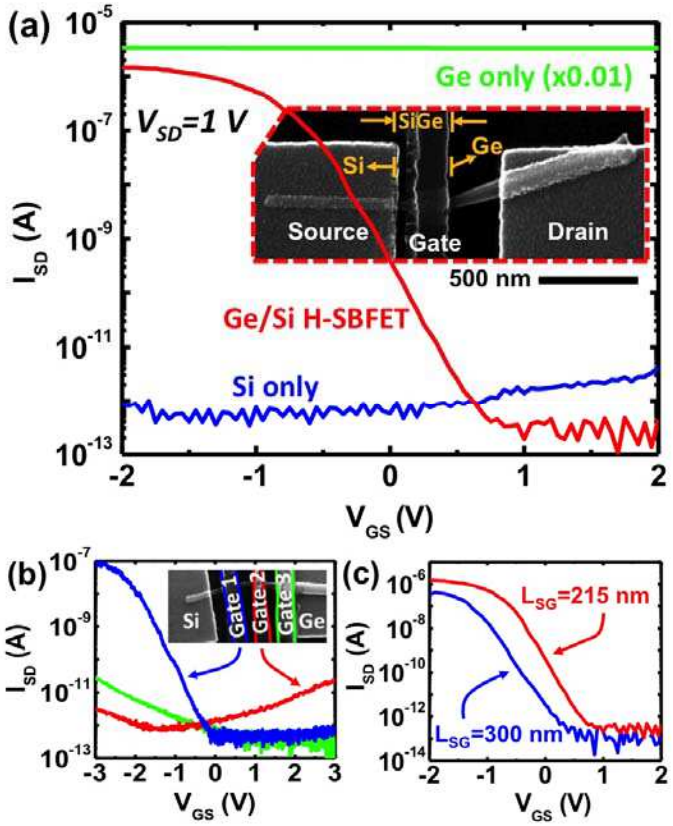

Figure 2. (a) Transfer characteristics of a Ge-Si axial NW heterostructure Schottky barrier FET contrasted to those obtained from pure Ge or pure Si grown simultaneously with the heterostrucrtured NW. The Ge-Si H-SBFET shows seven orders of magnitude current modulation compared to no modulation for its Si or Ge counterparts in the same gate-voltage range. Inset is an SEM image of the fabricated device. (b) Transfer curves from a H-SBFETs with multiple gates placed along the channel (inset SEM). The one closest to the Si source contact showed strongest modulation. (c) Transfer curves of single gated H-SBFETs with different spacing to the Si source showing stronger modulation when the gate is closest to the Si source contact. Reproduced from ref. [7] with permission.

Oppurtunities.

It is possible to utilize the built-in electric field in such axial Ge-Si devices for enhanced charge transport along the channel length of a field-effect transistor (FET). In addition, due to the compositional asymmetry, the Schottky barrier heights at both ends of such a NW can be different, as can be deduced from Fig. 1 (b). These asymmetries allowed for producing enhanced heterostructure Schottky barrier FET (H-SBFET) transfer curves as shown in Figure 2 (a) when compared to its homogenous counterparts (7). By placing multiple gates along the channel of the H-SBFET or changing the gate-source spacing on the Si segment of the NW, it was shown that this particular device operates as an H-SBFET (Fig. 2 (b-c)). However, as pointed out above, scaling of such device to nm scale lengths will not benefit from such performance gains.

Radial 1D Heterostructures

More abrupt doping and composition heterointerfaces can be obtained by utilizing the VLS mode to grow 1D NWs and altering the growth conditions to perform thin-film like conformal shell deposition on its sidewalls. Lauhon et al. first pioneered this growth in the Ge/Si material system (8). We developed a growth procedure to enable the in-situ growth of single crystal Ge/Si core/shell NWs without post-growth chemical or thermal treatments (9,10) and assessed the impact of such growth procedure on the transport properties of these heterostructured NWs (10). Excellent current drives and hole transport characteristics were demonstrated on such material system by Xiang and Wu (11, 12).

One potential of these core/shell heterostructures is in the area of strain engineering to enhance transport or emission properties of involved materials or extending their critical dimensions during heteroepitaxy (13). To lay down the framework for such device engineering, one needs to first identify the critical thicknesses for 1D NWs and understand the strain relaxation mechanisms. Our in-situ growth procedure enabled direct measure of these critical dimensions and examination of their strain relaxation mechanisms. We use a 15 nm radius Ge NW core and vary the Si shell thickness to provide the first measurement for a critical thickness in core/shell heteroepitaxy. Figure 3 shows TEM images for Ge/Si core/shell NWs with different shell thicknesses from 2 nm to 5 nm. As the shell thickness increases from 1 nm (not shown here) to 2.7 nm, a coherently strained structure is obtained. As the shell thickness increases beyond 3 nm, we observe a periodic pattern of extra (111) planes in the Si shell indicating the presence of dislocation loops to relieve axial strain in these core/shell NWs. From Fig. 3, we identify that the first critical thickness for strain relief in a Ge/Si core/shell NW is 3 nm for a 15 nm radius Ge NW.

A thorough investigation of the type of these dislocation loops have shown that they correspond to perfect type dislocation loops with a/2<110> Burger's vector, and have more impact on axial strain relief at the interface between two {110} facets. We have observed the gliding of such dislocation loops on {111} glide planes during in-situ heating experiments and confirmed their presence in cross-sections of the NWs. A forthcoming article in the journal of Nano Letters (14) will provide further details on critical dimensions and strain relief in core/shell Ge/Si NWs.

Conclusions

We provided a brief overview of our recent work in 1D heterostructures, and highlighted some of the challenges that face their deployment for device applications. We also highlighted their potential in emerging areas such as asymmetric field-effect transistor devices and their use for strain engineering and as compliant substrates.

Acknowledgments

We would like to acknowledge the substantial contributions and guidance of Dr. S. T. Picraux for this work, Dr. Wei Tang for assisting in TEM imaging and analysis, and John

Nogan for help in the integration laboratory at the Center for Integrated Nanotechnologies. This work was performed, in part, at the Center for Integrated Nanotechnologies, a U.S. Department of Energy, Office of Basic Energy Sciences user facility at Los Alamos National Laboratory (Contract DE-AC52-06NA25396) and Sandia National Laboratories (Contract DE-AC04-94AL85000). We thank the LDRD office at Los Alamos National Laboratory for providing financial support for this work.

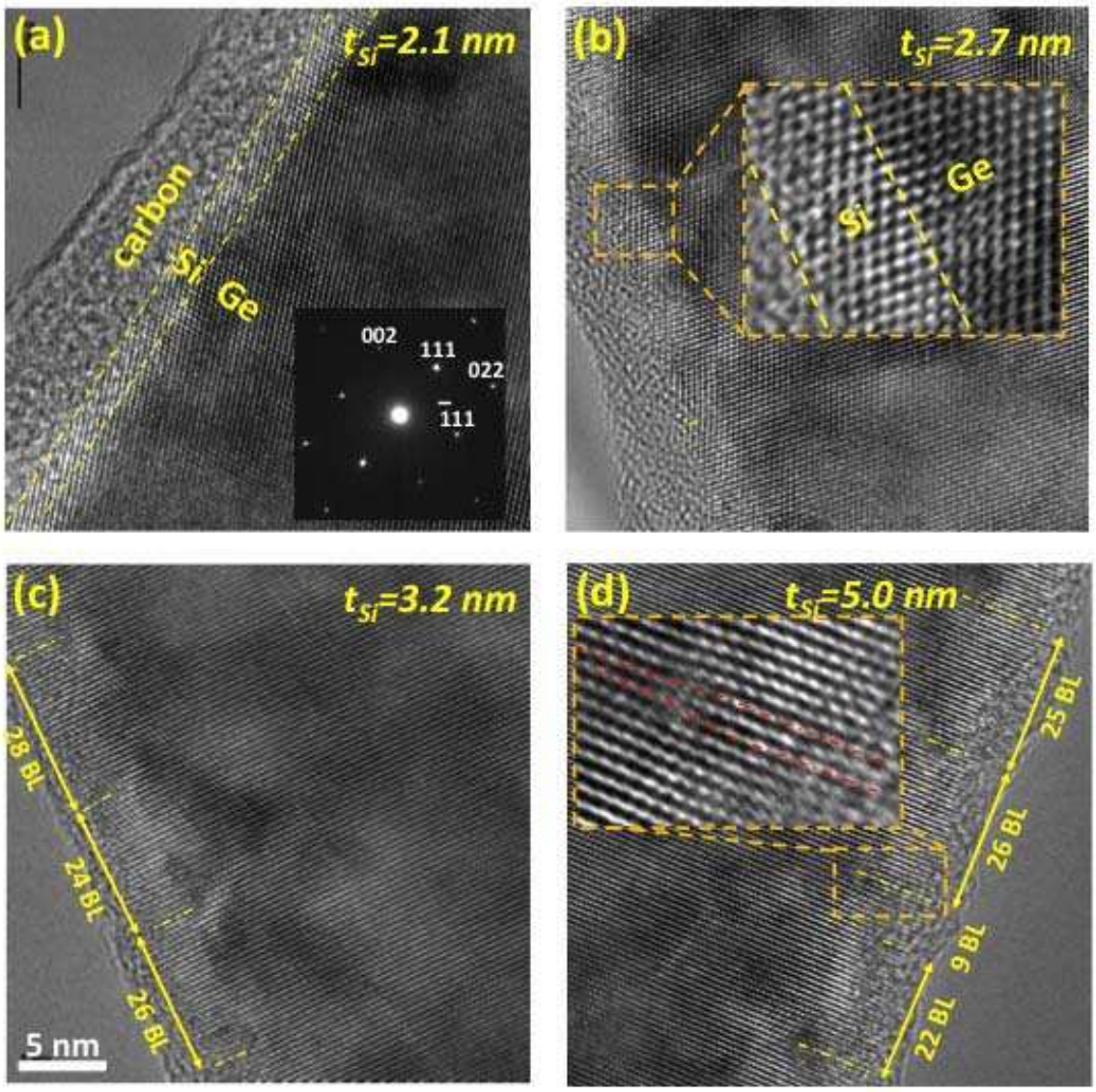

Figure 3. (a) 2.1 nm thick Si shell with corresponding selective area diffraction pattern showing single crystal core-shell structure with [111] growth axis. The outermost carbon shell develops during electron beam irradiation in TEM. (b) 2.7 nm thick Si shell case. The yellow dash-dot lines mark extra (111) planes in the Si shell where two random additional (111) planes were identified in this image. Inset is a zoom-in view at the Ge/Si interface. (c) 3.2 nm thick Si shell with a relative periodic pattern of extra (111) planes in the Si shell, where the number of (111) bi-layers (BL) between these extra (111) planes is indicated. (d) 5 nm thick Si shell case with similar periodicity of the extra (111) planes as in (c). Inset is a magnified image at the Ge/Si interface showing the extra (111) plane in the Si shell surrounded by the red dash-dot lines of the epitaxial (111) planes from core to shell.

References

1. F. Glas, *Phys. Rev. B*, **74**, 121302(R) (2006).
2. R. S. Wagner and W. C. Ellis, *Appl. Phys. Lett.*, **4**, 89 (1964).
3. E. I. Givargizov, Highly Anisotropic Crystals, p. 172-173, Springer-Verlag, New York, LLC (1986).
4. Y. Wu, R. Fan, and P. Yang, *Nano Lett.*, **2**, 83 (2002).
5. S. A. Dayeh, J. Wang, N. Li, J. Y. Huang, A. V. Gin, and S. T. Picraux, *Nano Lett.*, **11**, 4200 (2011).
6. D. E. Perea, N. Li, R. M. Dickerson, A. Misra, and S. T. Picraux, *Nano Lett.*, **11**, 3117 (2011).
7. S. A. Dayeh, R. M. Dickerson, S. T. Picraux, *Appl. Phys. Lett.*, **99**, 113105 (2011).
8. L. J. Lauhon, M. S. Gudiksen, D. Wang, and C. M. Lieber, *Nature*, **420**, 57 (2002).
9. S. A. Dayeh, N. H. Mach, J. Y. Huang, and S. T. Picraux, *Appl. Phys. Lett.* **99**, 023102 (2011).
10. S. A. Dayeh, A. V. Gin, and S. T. Picraux, *Appl. Phys. Lett.* **98**, 163112 (2011).
11. J. Xiang, W. Lu, Y. Hu, Y. Wu, H. Yan, and C. M. Lieber, *Nature*, **441**, 489 (2006).
12. W. Lu, J. Xiang, B. P. Timko, Y. Wu, and C. M. Lieber, *Proc. Nat. Acad. Sci.*, **102**, 10046 (2005).
13. S. Raychaudhuri, and E. T. Yu, *J. Vac. Sci. Tech. B* **24**, 2053 (2006).
14. S. A. Dayeh, W. Tang, H. Zheng, J. Wang, N. H. Mack, G. Swadener, K. L. Kavanagh, J. Y. Huang, K.-N. Tu, and S. T. Picraux, *submitted to Nano Lett.* (2012).